Modeling Bacterial Clearance Using Stochastic-Differential Equations

Ashraf Atalla[1], Aleksandar Jeremic[1]
[1]Department of Electrical & Computer Engineering
McMaster University, Hamilton, ON, Canada

***Abstract*— Capillary - tissue fluid exchange is controlled by the blood pressure in the capillary and the osmotic pressure of blood (pressure of the tissue fluid outside the capillaries). In this paper, we develop a mathematical model to simulate the movement of bacteria into and within a capillary segment. The model is based on Fokker-Planck equation and Navier-Stocks equations that accounts for different boundary conditions. Also, we model the transportation through capillary walls by means of anisotropic diffusivity that depends on the pressure difference across the capillary walls. By solving the model with a numerical method, it was possible to predict the concentration of bacteria at points within the capillary. However, numerical analysis consumes computational time and resources. To efficiently simulate the bacterial clearance, we propose a segmentation model that is based on breaking the capillary network into smaller sections with pre-defined properties in order to reduce the overall computational time. The proposed model shows a great reduction in computational time and provides accurate results when compared to the numerical analysis.**

I. INTRODUCTION

The capillary network is a complex-interconnected structure. A single blood cell traveling from the arteriole to a venule via a capillary bed passes through, on average in the respiratory system, $40-100$ capillary segments [1]. The cardiovascular systems responsible of delivering blood to the tissue under sufficient pressure to exchange materials. This is a two way process, at which nutrients, Oxygen, and other materials are carried to the tissue and cells during the outflow. On the other hand, blood is returned along with the wastes of cellular metabolism during the return flow.

There are three mechanisms whereby capillary exchange can occur, diffusion, bulk flow, and vesicular transport. It is necessary to have an accurate model for the capillary-tissue exchange mechanism. This can be useful in many applications such as understanding the dispersion of drug particles, through vascular system, in human tissue [2], [3] as well as understanding the behavior of bacterial dispersion [4] and and the factors influencing its clearance [5], [6], [7], [8].

Modeling the exchange process can be carried by means of coupling the classical diffusion (Fick's law) with Navier-Stokes equations. However, for a small number of particles, classical diffusion fails to introduce a satisfactory representation of the particle dispersion. It has been observed that the patterns of drug dispersion in human body organs exhibit certain irregularities (discontinuities) which can not be modeled with Fick's law of diffusion even using anisotropic and nonhomogeneous diffusivity. In order to accurately model the exchange process, we propose a stochastic based model of the diffusion process based on the well known Fokker Planck equation [9]. In order to account for the different mechanisms whereby capillary exchange can occur (diffusion and bulk flow), we model the capillary walls with means of pressure-dependent anisotropic diffusivity with slip conditions for the plasma flow inside the capillary. The main advantage of this technique lies in the fact that it accounts for both drift and random effects such as Brownian motion which are not accounted for in commonly used classical techniques based on Fick's law of diffusion. The extension to realistic geometry is straight forward since it can be dealt with using Finite Element Method.

This paper is organized as follows. First, we introduce the flow model using Navier-Stokes equations. Next, we utilize Fokker Planck equation with convection field to represent the probability function of the position of a particle (i.e, single bacteria) in the capillary-tissue region. Then, we compute the probabilities of absorption and transmission (clearance) of a single particle and utilize it to construct the segmentation model. Finally, we compute the probability mass function (PMF) of the total number of bacterial particles.

II. CAPILLARY BLOOD FLOW MODEL

Many attempts are done to study the motion of blood though a capillary segment[10] – [13]. In this paper we present a stochastic model for capillary exchange. First, we consider a three dimensional circular cylindrical tube, representing a capillary segment of radius R and finite length L with permeable wall to promote fluid exchange across the wall. The equations of momentum and continuity are given by

$$\overbrace{\rho\Big(\underbrace{\frac{\partial \mathbf{u}}{\partial t}}_{\substack{\text{Unsteady}\\ \text{acceleration}}} + \underbrace{\mathbf{u}\cdot\nabla\mathbf{u}}_{\substack{\text{Convective}\\ \text{acceleration}}}\Big)}^{\text{Inertia (per volume)}} = \overbrace{\underbrace{-\nabla p}_{\substack{\text{Pressure}\\ \text{gradient}}} + \underbrace{\mu\nabla^2\mathbf{u}}_{\text{Viscosity}}}^{\text{Divergence of stress}} + \underbrace{\mathbf{f}}_{\substack{\text{Other}\\ \text{body}\\ \text{forces}}} \quad (1)$$

$$\nabla\cdot\mathbf{v} = 0 \quad (2)$$

†jeremic@mcmaster.ca
‡ashraf.atalla@gmail.com
This work has been supported by National Research Council Canada

Capillary specifications	
L	$1mm$
R	$1\mu m$
ρ	$1025kg/m^3$
μ	$0.0015Ns/m^2$ at 37°
$p_{artriole\ end}$	$40mmHg$
$p_{vanule\ end}$	$15mmHg$
p_i	$-6mmHg$
ρ_c	$25mmHg$
ρ_i	$5mmHg$
L_c	$28.6*10^{-7}cm/(s\cdot cmH_2O)$, $cmH_2O=0.098KPa$
ϕ	0 and 0.15

TABLE I: Capillary specifications.

where ρ is the plasma fluid density, μ is the viscosity, p is the hydrostatic capillary blood pressure, and $\mathbf{u}$ is the velocity vector.

The radial velocity u_r is governed by Starling's law which is a mathematical model for fluid movement across capillaries, given by

$$u_r = K[(p-p_i)-(\rho_c-\rho_i)] \tag{3}$$

where, K is the filtration constant which is the product of the capillary surface area (A) and the capillary hydraulic conductance (L_c), i.e., $K=AL_c$. p_i is the hydrostatic interstitial hydrostatic fluid pressure, ρ_c is the capillary oncotic pressure (osmotic pressure of the plasma proteins), and ρ_i is the tissue oncotic pressure (osmotic pressure of the proteins in the interstitial fluid).

Note that, in the previous equation, $[(p-p_i)-(\rho_c-\rho_i)]$ represents the net driving pressure for filtration. The corresponding boundary conditions are

$$\phi\frac{\partial u_z}{\partial r}+u_z=0 \qquad at\ \ r=R \tag{4}$$

$$u_r=\frac{K\mu}{R}\left(\frac{p}{\rho_c-\rho_i+p_i}-1\right) \qquad at\ \ r=R \tag{5}$$

$$p=p_a \qquad at\ \ z=0 \tag{6}$$

$$p=p_v \qquad at\ \ z=L \tag{7}$$

The boundary condition (7) is the Beavers and Joseph condition while (7) results from Starling's law, where $\phi=\sqrt{k}/\delta R$, δ is the slip parameter and k is the specific permeability of the poros medium. (7) reduces to the no-slip condition when $k=0$. Also, p_a and p_v are the pressures at the arterial and venous ends, respectively.

We solve the above model using Finite Element package (COMSOL Multiphysics) for a capillary segment with specifications defined in Table (I).

In Figure (1), we show the axial velocity field profile along the radial direction at the center of the capillary. Observe that the axial velocity increases as the slip coefficient (ϕ) increases and vice versa. Moreover, it coincides with the no-slip condition when $\phi=0$. In figure (2), we illustrate the variation of axial velocity along the axis $r=0$ for different ϕ. It is observed that u_z has a concave profile downwards with a minimum around the center of the capillary segment. In Figure (3), we show the pressure along the capillary segment, observe that the blood pressure almost has a linear relation with the capillary-segment length. The deviation from linearity is due to the introduction of the permeable wall condition in (7). This relation is very important in this context and will be utilized in Section IV.

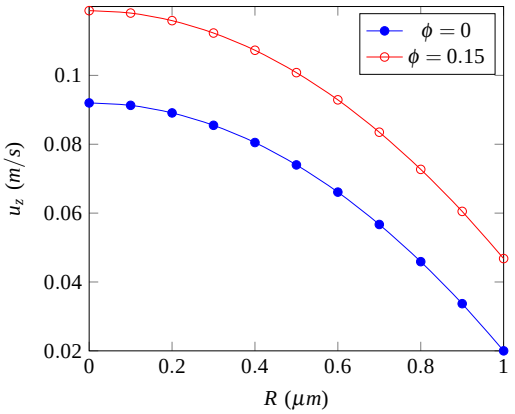

Fig. 1: Axial velocity profile at $z=L/2$ for different slip coefficients.

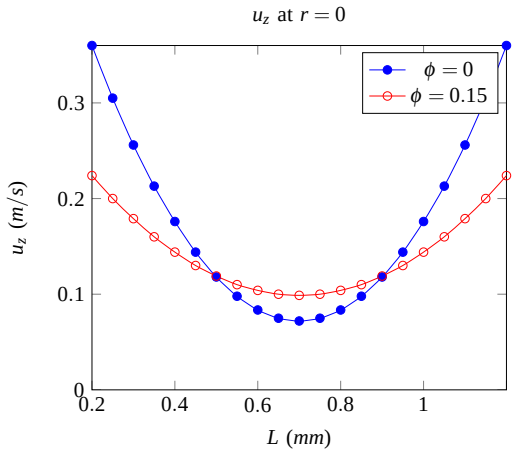

Fig. 2: Axial velocity profile along the axis $r=0$ for different slip coefficients.

III. Modeling the Exchange Process

In order to model the dispersion of particles through and inside a capillary segment, let us assume that at an arbitrary time t_0 we introduce n_0 (or equivalently concentration c_0) particles at location r_0 being at the beginning of the capillary segment. When the number of particles is large macroscopic approach corresponding to the Fick's law of diffusion is adequate for modeling the transport phenomena. However, to model the motion of the particles when their number is small a microscopic approach corresponding to stochastic differential equations (SDE) is required. The diffusion process for the transport of particle in an open environment is given by the itõ stochastic differential equation:

$$dX_t=\mu(X_t,t)dt+\sigma(X_t,t)dW_t \tag{8}$$

where X_t, in R^3, is the location and W_t is a standard Wiener process in R^3.

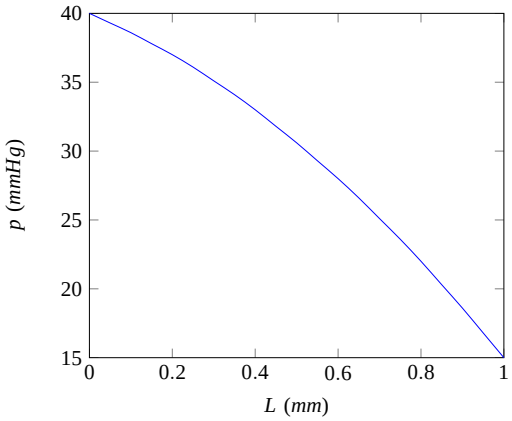

Fig. 3: Pressure profile along the axis $z = 0$ of a capillary segment.

The function $\mu(X_t,t)$ is referred to as the drift coefficient while $\sigma()$ is called the diffusion coefficient such that in a small time interval of length dt the stochastic process X_t changes its value by an amount that is normally distributed with expectation $\mu(X_t,t)$dt and variance $\sigma^2(X_t,t)$dt and is independent of the past behavior of the process.
Assuming three-dimensional environment $r = (x_1,x_2,x_3)$, we compute the probability density function, $f(r,t)$, of one particle occupying space around r at time t using the Fokker-Planck equation [9]

$$\frac{\partial f(r,t)}{\partial t} = \left[-\sum_{i=1}^{3} \frac{\partial}{\partial x_i} D_i^1(r) + \right. \\ \left. + \sum_{i=1}^{3}\sum_{j=1}^{3} \frac{\partial^2}{\partial x_i \partial x_j} D_{ij}^2(r) \right] f(r,t) \qquad (9)$$

where partial derivatives apply the multiplication of D and $f(r,t)$, D^1 is the drift vector and D^2 is the diffusion tensor given by

$$\begin{aligned} D_i^1 &= \mu \\ D_{ij}^2 &= \frac{1}{2}\sum_l \sigma_{il}\sigma_{lj}^T \end{aligned} \qquad (10)$$

In the case of anisotropic diffusivity, the diffusivity tensor is defined by a 3×3 matrix. We can understand the geometry of anisotropic diffusion by looking at the eigenvalue decomposition of D.

$$\mathbf{D^2} = \mathbf{X}\Lambda\mathbf{X}^{-1} \qquad (11)$$

where $\mathbf{X} = [e_1 e_2 e_3]$, e_i are the eigenvectors of $\mathbf{D^2}$ and $\Lambda = \begin{bmatrix} \lambda_1 & 0 & 0 \\ 0 & \lambda_2 & 0 \\ 0 & 0 & \lambda_3 \end{bmatrix}$. λ_1,λ_2, and λ_3 are the eigenvalues of $\mathbf{D^2}$.

The eigenvalues are real, mutually orthogonal, and positive. When $\lambda_1 = \lambda_2 = \lambda_3$, the diffusion process is considered isotropic and the observable contour of $f(r,t)$ forms a sphere, as explained previously. In general, the contour of $f(r,t)$ forms and ellipsoid with the following function

$$\frac{x^2}{{\lambda_1}^2} + \frac{y^2}{{\lambda_2}^2} + \frac{z^2}{{\lambda_3}^2} = 1 \qquad (12)$$

For the bounded domain, (9) can be easily solved, numerically using following boundary conditions

$$f(r,t) = 0 \qquad \text{for absorbing boundaries} \qquad (13)$$

$$\hat{\mathbf{n}} \cdot \nabla f = 0 \qquad \text{for reflecting boundaries} \qquad (14)$$

where $\hat{\mathbf{n}}$ is the normal vector to the boundary.
The diffusion model does not only include the inner region of the capillary, but also the surrounding tissues, the arterial end, and the proceeding parts of the capillary network. The coupling between the flow model and the diffusion-convection equations is achieved by implementing domain and boundary conditions as follows:
Domain Configuration

- Capillary inner domain: we use homogenous diffusivity with a convection flux corresponding to the velocity field, $\mathbf{u}$, calculated in II, i.e., $\mu = \mathbf{u}$ and $\mathbf{D^2} = DI_3$
- Capillary wall: only convection flux in the radial direction is considered with anisotropic diffusivity with the eigenvalues $\lambda_1 = \beta cos(\theta)$, $\lambda_2 = \beta sin(\theta)$, and $\lambda_3 = 0$ where β is a scaling factor that is a function of pressure difference, i.e. $\beta = sign(p - \rho_c)$. This representation of the diffusivity tensor allows diffusion only in the radial direction.

Boundary Configuration

- Capillary inner wall: we use the continuity condition.
- Capillary outer wall: we propose an absorbing boundary condition to enforce absorbtion of all the particles leaving the capillary to the surrounding tissues.
- Arteriole end: we assume a reflecting boundary in order to prevent all particles from re-entering the arteriole.
- Venule end: we assume an infinite domain with continuity condition in between.

Then, the probability density function is calculated in the proposed geometry using COMSOL Multiphysics. In Figure (4) we show the time evolution of the particle pdf inside a capillary segment assuming that the particle starts moving from the arterial end. In order to study the behavior of the capillary network, we study two main probabilities:

1) P_A: The probability of a particle to get absorbed into the surrounding tissues.
2) P_T: The probability of a particle to get transmitted to the proceeding capillary network.

In Figure 4, we present P_A as a function of time. Observe that, the probability of absorbtion increases with time as the particle moves along the capillary segment while reaches an upper bound (saturation) as it moves to the rest of the capillary bed ($t_{sat} \approx 2 * 10^{-5} sec$). The plot in Figure (9b) shows the time function of P_T. Similarly, the probability of transmission reaches an upper bound as it moves to the rest

of the capillary bed. Moreover, P_T shows a delay response due to the time required by a particle to hit the venule end of the capillary.

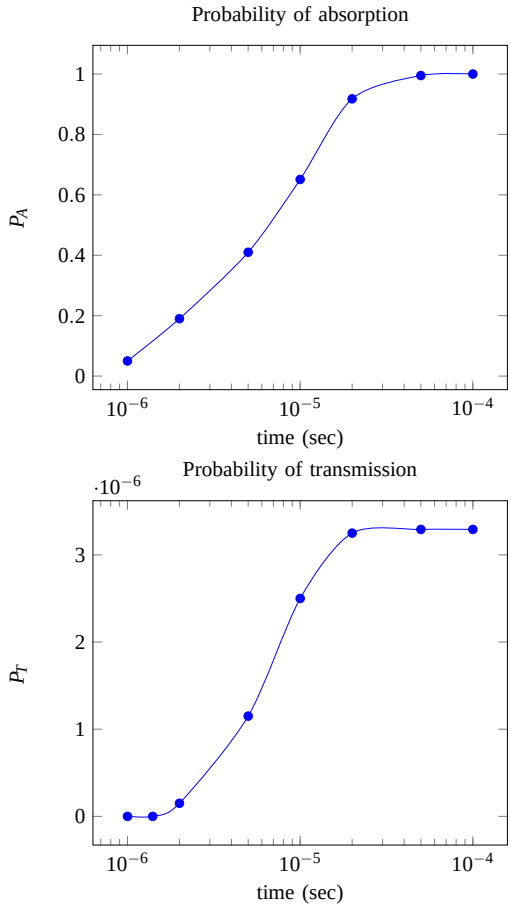

Fig. 4: Evolution of the probabilities of absorption and transmission of a single particle traveling from the arteriole to a venule via a capillary segment.

IV. Segmentation Model of the Capillary Network

In this section, we propose a time efficient technique, segmentation model (SM), to calculate the aforementioned absorption and transmission probabilities (P_A and P_T, respectively) which can be used for a complex capillary network. The main idea of this technique is breaking the capillary network into smaller sections with pre-defined properties in order to reduce the overall computational time. Ahead, we present the main steps to implement the proposed algorithm:

- Step 1: discritization of the capillary into a large number of smaller sections.
- Step 2: calculating the P_A and P_T of each section as a function of pressure.
- Step 3: integrating over the capillary network.

First, we start by discretizing the previously introduced capillary segment into n smaller sections, as shown in Figure (6). Next, we calculate P_{A_i} and P_{T_i}, namely, the absorption and

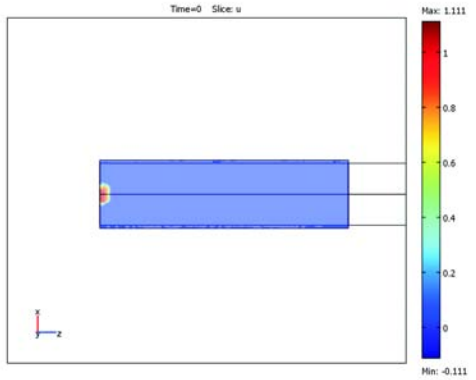

(a) t=0 sec

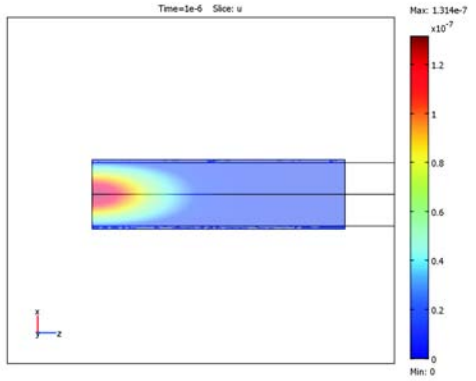

(b) t=10^{-6} sec

Fig. 5: Evolution of $f(r,t)$ inside a capillary segment.

transmission probabilities within the i^{th} section, where $i = 1,\cdots,n$. This is done separately for each section under the same conditions calculated in Section II, i.e., the pressure along each section is set to the values corresponding to those in Figure (3). The pressure at the beginning of i^{th} section is defined as p_{i-1} and its pressure drop is $\triangle p_i$ with p_0 is the maximum pressure at the arteriole end and p_n is the minimum pressure at the venule end. Also, we assume that the diffusive particle starts its movement from the beginning of each section.

In Figures (7 and 8), we illustrate the probabilities of absorption and transmission, respectively, of each section as a function of capillary blood pressure. The calculations are done for $n = 20$ sections at 1.01μ *sec*. As expected, P_{A_i} decrease as moving along the capillary segment since, in principle, the absorption on the capillary walls depends on the pressure difference across the wall which decreases as moving towards the venule end. However, P_{T_i} shows a minima near the middle of the capillary segment since it mainly depends on the axial velocity of the blood which has a minima near the middle of the capillary as well.

This discrete representation of the probabilities of each section is very useful in calculating the total absorption or transmission probabilities for a general capillary segment. For better understanding of the importance of Figures (7 and 8) we show an example of calculating the total absorption

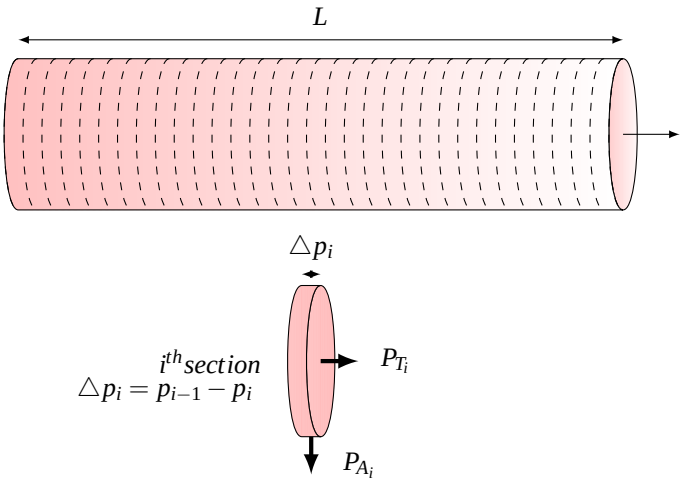

Fig. 6: Discritization of a capillary segment.

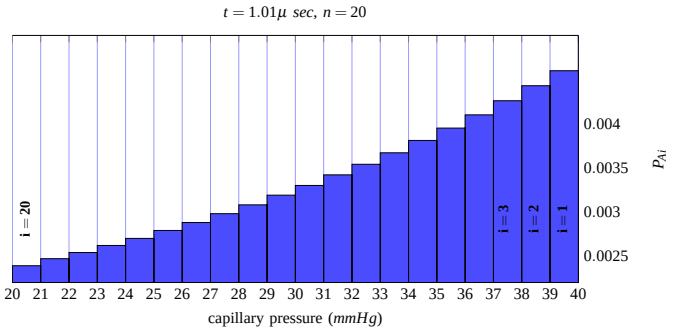

Fig. 7: Probability of absorption of the i^{th} capillary section, for $i = 1, \cdots, n$, as a function of capillary blood pressure.

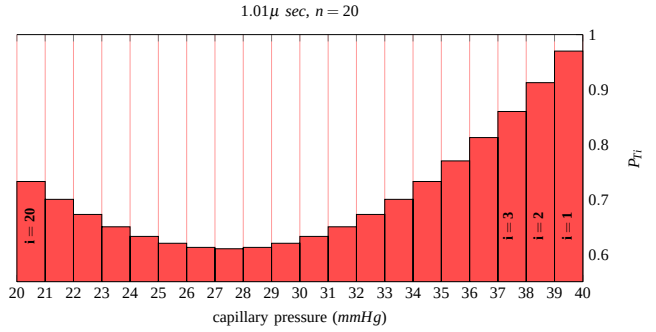

Fig. 8: Probability of transmission of the i^{th} capillary section, for $i = 1, \cdots, n$, as a function of capillary blood pressure.

and transmission probabilities for a capillary segment consisting of n sections with known starting pressure and length. Also, for simplicity, we assume that the section length is equal to that presented in Figures (7 and 8). We first define the different probabilities that will be used in the example below.

$P_{A_i,t}$, the absorption probability of the i^{th} section at time t for a particle starting from the same section.

$P_t^{A_i}$, the absorption probability of the i^{th} section at time t for a particle starting from the 1^{st} section.

$P_{tot,t}^{A_i}$, the total absorption probability of the sections $1, \cdots, i$ at time t for a particle starting from the 1^{st} section.

$P_{T_i,t}$, the transmission probability of the i^{th} section at time t for a particle starting from the same section.

$P_{tot,t}^{T_i}$, the total transmission probability from the sections $1, \cdots, i$ at time t for a particle starting from the 1^{st} section. Also, equal to $P_t^{T_i}$.

It can be shown that the total probabilities, of absorption and transmission, for n sections at time t_k are given by

$$P_{tot,t_k}^{A_n} = \sum_{i=1}^{n} P_{t_k}^{A_i} \tag{15}$$

$$P_{tot,t_k}^{T_i} = P_{t_k}^{T_i} = \sum_{j=1}^{k} (P_{tot,t_j}^{T_{i-1}} - P_{tot,t_{j-1}}^{T_{i-1}}) P_{T_i,t_j} \tag{16}$$

where

$$P_{t_k}^{A_i} = \sum_{j=1}^{k} (P_{tot,t_j}^{T_{i-1}} - P_{tot,t_{j-1}}^{T_{i-1}}) P_{A_i,t_j} \tag{17}$$

In order to validate the proposed algorithm, we illustrate,in Figure (9), the total absorption and transmission probabilities for a capillary segment similar to the one studied previously in Section III and compare our results to the results obtained using the Finite Element solver. The capillary segment is divided into 50 sections. It is obvious that the results obtained using the segmentation model are very accurate and close to those obtained by the Finite Element solver. Also, the computational time required for implementing our model (using MATLAB) is $7.8474 * 10^{-4}$ *sec* which is greatly less than the time required by the Finite Element solver (4.4 *hrs*). Moreover, the segmentation algorithm can be easily used to model complex capillary network since it can be divided into smaller sections that will be later integrated.

V. Modeling the Exchange of Multiple Particles

In this section we model the exchange probabilities (absorption and transmission) of multiple particles entering a capillary network. Let n_0 be the initial number of particles entering a capillary network that has an absorbing and transmission probabilities of $P_{A,t_j} \equiv P_{tot,t_j}^{A_n}$ and $P_{T,t_j} \equiv P_{tot,t_j}^{T_n}$, respectively. Hence, the probability that there are n absorbed particles within the network at time t_j becomes

$$\mathrm{P}_j(n) = \binom{n_0}{n} P_{A,t_j}^n (1 - P_{A,t_j})^{n_0 - n} \quad n = 1, \ldots, n_0 \tag{18}$$

Similarly, the probability that there are m transmitted particles within the network at time t_j is

$$\mathrm{P}_j(m) = \binom{n_0}{m} P_{T,t_j}^m (1 - P_{T,t_j})^{n_0 - m} \quad m = 1, \ldots, n_0 \tag{19}$$

Finally, The joint probability of n absorbed and m transmitted particles is given by

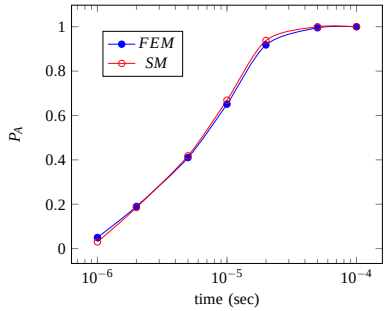

(a) Probability of absorption

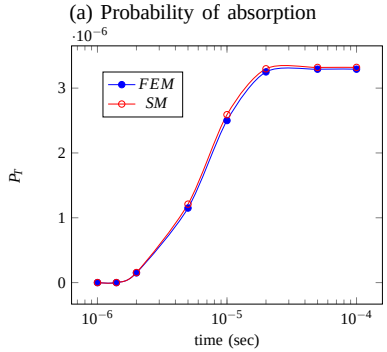

(b) Probability of transmission

Fig. 9: Comparison of the Finite Element and Segmentation Methods in calculating P_A and P_T.

$$\mathrm{P}_j(m,n) = \binom{n_0}{m}\binom{n_0-m}{n} P_{T,t_j}^m P_{A,t_j}^n (1-P_{A,t_j}-P_{T,t_j})^{n_0-m-n} \tag{20}$$

where $m+n=1,\ldots,n_0$

VI. Conclusions

Oka and Murata [10] studied the steady motion of blood through the capillary wall using a linear model of the blood flow and utilizing Starling's law, that is, the rate of flow per unit area across the the wall boundary is directly proportional to the pressure difference across the wall. However, Strivastava [11] showed that the linearized model fails to give an adequate representation of the flow field, especially in short vessels. Oka's linear model has been extended to the non-linear case by Mariamma and Maghi [12]. They considered the steady laminar flow of the blood as a homogeneous Newtonian fluid in tube with permeable wall. Elshahed [13] studied the effect of exchange of fluid across the capillary wall on the flow of blood with slip velocity and proposed a closed form the velocity fields. In this work, we solve the set of equations provided by Elshahed numerically, in order to compute the velocity field through the capillary.

In this paper we modeled the capillary exchange using stochastic diffusion embedded into Newtonian flow of the blood. To the best of our knowledge it is a first attempt to model the exchange process in as a random, diffusive process. As a consequence our model is more realistic with respect to modeling of the absorption rate as it it take into account capillary size, velocity of blood flow and diffusivity of a particular bacteria, drug, etc. In addition we demonstrated ability to perform computationally intensive procedures in an efficient way using segmented approach. The main focus of future work should be experimental validation of the proposed models.

References

[1] C. Doerschuk, "Leukocyte trafficking in alveoli and airway passages," *Respiratory Research*, vol. 1, no. 3, p. 136, 2000.

[2] H. Terayama, K. Okumura, K. Sakai, K. Torigoe, and K. Esumi, "Aqueous dispersion behavior of drug particles by addition of surfactant and polymer," *Colloids and Surfaces B: Biointerfaces*, vol. 20, no. 1, pp. 73–77, 2001.

[3] Y. Yano, K. Yamaoka, Y. Aoyama, and H. Tanaka, "Two-compartment dispersion model for analysis of organ perfusion system of drugs by fast inverse Laplace transform (FILT)," *Journal of Pharmacokinetics and Pharmacodynamics*, vol. 17, no. 2, pp. 179–202, 1989.

[4] P. Cannon, F. Sullivan, and E. Neckermann, "Conditions influencing the disappearance of living bacteria from the blood stream," *Journal of Experimental Medicine*, vol. 55, no. 1, pp. 121–137, 1932.

[5] G. Green and E. Kass, "Factors influencing the clearance of bacteria by the lung," *Journal of Clinical Investigation*, vol. 43, no. 4, p. 769, 1964.

[6] J. Holman, K. Burnett, and L. Burnett, "Effects of hypercapnic hypoxia on the clearance of Vibrio campbellii in the Atlantic blue crab, Callinectes sapidus Rathbun," *Biological bulletin*, pp. 188–196, 2004.

[7] J. Pollard Jr, "Material and method for removing immunoglobulins from whole blood," Aug. 7 1984, uS Patent 4,464,165.

[8] D. Rogers, "Host mechanisms which act to remove bacteria from the blood stream," *Microbiology and Molecular Biology Reviews*, vol. 24, no. 1, pp. 50–66, 1960.

[9] H. Risken, *The Fokker-Planck equation: Methods of solution and applications*. Springer, 1989.

[10] S. Oka and T. Murata, "A theoretical study of the flow of blood in a capillary with permeable wall," *Jap. J. Appl. Phys*, vol. 9, pp. 345–352, 1970.

[11] L. Srivastava and V. Srivastava, "On two-phase model of pulsatile blood flow with entrance effects," *Biorheology(Oxford)*, vol. 20, no. 6, pp. 761–777, 1983.

[12] N. Mariamma and S. Majhi, "Flow of a newtonian fluid in a blood vessel with permeable wallA theoretical model," *Computers and Mathematics with Applications*, vol. 40, no. 12, pp. 1419–1432, 2000.

[13] M. El-Shahed, "Blood flow in a capillary with permeable wall," *Physica A: Statistical Mechanics and its Applications*, vol. 338, no. 3-4, pp. 544–558, 2004.